

# RSC Advances



This is an *Accepted Manuscript*, which has been through the Royal Society of Chemistry peer review process and has been accepted for publication.

*Accepted Manuscripts* are published online shortly after acceptance, before technical editing, formatting and proof reading. Using this free service, authors can make their results available to the community, in citable form, before we publish the edited article. This *Accepted Manuscript* will be replaced by the edited, formatted and paginated article as soon as this is available.

You can find more information about *Accepted Manuscripts* in the [Information for Authors](#).

Please note that technical editing may introduce minor changes to the text and/or graphics, which may alter content. The journal's standard [Terms & Conditions](#) and the [Ethical guidelines](#) still apply. In no event shall the Royal Society of Chemistry be held responsible for any errors or omissions in this *Accepted Manuscript* or any consequences arising from the use of any information it contains.

# Consistent double Gaussian model with non-symmetric potential barriers at contacts for organic diodes

Muhammad Ammar Khan,<sup>1</sup> Sun Jiu-Xun,<sup>1,2\*</sup> Jin Ke,<sup>2</sup> Cai Ling-Cang,<sup>2</sup> and Wu Qiang<sup>2</sup>

<sup>1</sup> School of Physical Electronics, University of Electronic Science and Technology, Chengdu 610054, China

<sup>2</sup> Laboratory for Shock Wave and Detonation Physics Research, Southwest Institute of Fluid Physics, Mianyang 621900, China

\* Corresponding author. E-mail address: sjx@uestc.edu.cn

**Abstract:** A transport model with double Gaussian density of state (DOS) for organic semiconductors is proposed, with one Gaussian DOS for free carriers and one for trapped carriers. The variations of the density of trapped carriers with the density of free carriers, the effective mobility and ratio of diffusion coefficient to effective mobility with the density of trapped carriers are analyzed. It is shown that the ratio of diffusion coefficient to effective mobility is the Einstein type for free carriers, the ratio for total carriers is the non-Einstein type, and is an increasing function of the density of trapped carriers at low density, decreasing function at high density. The importance of non-symmetric barriers at contacts is emphasized to quantitatively describe the current-voltage relationships of typical organic layers sandwiched in two metallic electrodes. It is shown that slopes of current-voltage curves at low bias are very sensitive to the values of right barriers. The slopes in all bias are sensitive to the values of left barriers, and would increase as the left barrier decreasing. As applying the modified model to three organic diodes, the excellent agreement between theoretical results and experimental data is obtained.

**Keywords:** organic diode, non-symmetric barriers, Gauss traps, Einstein relationship

**PACS:** 72.80.Le; 73.40.-c; 73.40.Cg; 73.61.Ph; 85.60.Bt

## 1. Introduction

The research of the optoelectronic and electrical transport properties in conjugated semiconducting polymers has drawn intensive attention because of their potential applications in organic semiconductor devices such as light-emitting diodes (LEDs) and field-effect transistors (FETs) [1-18]. Understanding their charge-carrier transport properties is very useful to improve the device performances, design and synthesize better materials. It was demonstrated that the current in single carrier diodes with amorphous polymer layers sandwiched by two electrodes is space-charge limited (SCL) [1-18].

Dauids et al. [1] proposed a unified device model considering two types of carriers for single layer organic LEDs, and Crone et al. [2] extended it into bilayer diodes. They also studied the impact of local electric fields on the injection barrier. Koster et al. [3] proposed a model for organic solar cells considering two types of carriers. However, the most organic diodes are single type of carriers, the SCL current in organic diodes is described by the solutions of drift and Poisson equations, with different expressions of mobility. The density dependent mobility of Vissenberg and Matters (VM) [4] is popular, which is originated from hopping in an exponential density of states (DOS). This description has been used to unify the charge transport in FETs and LEDs [5-7]. Pasveer *et al.* [8] developed a description for the mobility incorporating both the density and field dependence, based on charge-carrier hopping within the Gaussian DOS. The mobility of Pasveer *et al.* has been widely applied to describe current-voltage ( $J$ - $V$ ) relationships of organic devices by many authors [9-18].

Van Mensfoort *et al.* [11] and we [12,13] have numerically solved drift-diffusion model (DDM) and drift model by using parameters optimized by Pasveer *et al.* [8] for NRS-PPV and OC<sub>1</sub>C<sub>10</sub>-PPV. The obtained J-V curves are in good agreement with experimental data [9-13]. Zhou et al. [14] studied the effect of high carrier density to mobility by using Monte Carlo simulation. Coehoorn et al. [15, 16],

Bässler and Köhler [17] reviewed recent advances in charge transport in disordered organic semiconductors. Myers and Xue [18] reviewed organic semiconductors and their applications in photovoltaic devices, discussed the fundamental electronic nature of organic semiconductors, processing techniques, and their application to two main classes of optoelectronic devices, light emitting diodes, and photovoltaics.

However, Zhang *et al.* [19] demonstrated that electron transport is consistently described by the concept of free electrons in combination with deep traps. Recently Nicolai *et al.* [20, 21] analyzed the reason that both VM and Pasveer models provide a consistent description of the  $J$ - $V$  relationships of organic devices. The reason is that the section of the Gaussian DOS that is being filled during a  $J$ - $V$  scan may also be approximated by an exponential, or vice versa [20, 21]. Nicolai *et al.* [20, 21] further emphasized that the trapped carriers are very important for description of  $J$ - $V$  curves. If considering the trapped carriers with Gaussian DOS in the DDM and treating the mobility as a constant, the  $J$ - $V$  curves of many organic diodes can be qualitatively described. But the fitting procedure and values of parameters are not clearly presented and explained [20, 21].

Lange *et al.* [22] proposed a model for band bending in contacts of polymer layers with metallic electrodes. Cottaar *et al.* [23, 24] present a scaling theory for charge transport in disordered molecular semiconductors that extends percolation theory to the percolating one in the random resistor network representing charge hopping. A density dependent mobility for Miller-Abrahams and Marcus hopping on different lattices with Gaussian energy disorder are derived. Oelerich *et al.* [25] suggest a recipe on how to determine the density of states (DOS) in disordered organic semiconductors from the measured dependence of the charge carrier mobility on the concentration of carriers. The recipe is based on a theory for the concentration-dependent mobility. Fishchuk *et al.* [26] developed an analytical mobility model to

describe hopping transport in organic semiconductors including both energetic disorder and polaronic contributions due to geometric relaxation.

Bruyn *et al.* [27] derived an analytic approximate JV formula for organic diodes. In the derivation of the analytic formulae, the mobility has been treated as a function of temperature being independent to density and electric field. But the analytic formula cannot consider trapped carriers; and it merely describes JV data qualitatively. It is notable that Pasveer *et al.* [5], Bruyn *et al.* [27], and Nicolai *et al.* [20, 21] belong to the group of Blom. They have proposed about tens of models considering different physical effects, but the final model has not been found [3, 5, 8, 19-21, 27, 42].

Except for the traps, the barriers at contacts between organic layer and electrodes are important for quantitative description of JV data. Davids *et al.* [1] and Crone *et al.* [2] studied the impact of local electric fields on the injection barrier. Chen *et al.* [28] studied electrostatic field and partial Fermi level pinning at the pentacene-SiO<sub>2</sub> interface. Recently, Yogev *et al.* [29] and Oehzelt *et al.* [30] independently proposed Fermi level pinning is induced by gap states in organic semiconductors. Because the height of barriers is tightly related with Fermi levels, since the Fermi level in organic semiconductors is pinned, it implies the barriers almost are constant. Neumann *et al.* [31, 32] developed self-consistent theory of unipolar charge-carrier injection in metal/insulator/metal systems. They derived boundary conditions used for the drift-diffusion equations. The densities of electrons [31] or holes [32] are expressed as functions of barriers which are weakly dependent to electric field at interfaces. Thus, Bruyn *et al.* [27] directly adopted constant barriers in their derivation of an analytic JV formula.

In the DDM, the ratio between the diffusion coefficient  $D$  and the mobility  $\mu$  is given by the Einstein relationship (ER),  $D/\mu = k_B T/q$ . Some authors [33-36] proposed the ER should be replaced by the generalized Einstein relation (GER) with the ratio  $k_B T/q$  multiplied by a factor. However, Neumann *et al.*

[37] disapprove the GER through theoretical analysis. Wetzelaer et al. [38] confirmed the validity of the ER in organic semiconductors by studying the diffusion-driven currents of single-carrier diodes.

In this paper, we would present detailed formulation of DDM with Gaussian traps taken into account, give an explanation to the GER, and show that, except the Gaussian traps, the non-symmetric potential barriers at contacts also are important factor for quantitative description of J-V curves by applying the DDM to three typical diodes.

## 2. Fundamental Model

The fundamental energy-band model for p-type materials used in this paper is schematically plotted in Fig. 1. The model in Fig. 1 consist two Gaussian DOS. One Gaussian for free carriers and one for trapped carriers with widths  $\sigma$  and  $\sigma_t$ , center energy levels  $E_v$  and  $E_t$ , respectively.

$$D_f(E) = (N_0 / \sigma \sqrt{2\pi}) \exp[-(E - E_v)^2 / 2\sigma^2] \quad (1)$$

$$D_t(E) = (N_t / \sigma_t \sqrt{2\pi}) \exp[-(E - E_t)^2 / 2\sigma_t^2] \quad (2)$$

$N_0$  is the total concentration of states at energy levels  $E_v$ ,  $N_t$  is the total concentration of traps. The densities of free and trapped holes can be expressed as

$$p_f = \int_{-\infty}^{\infty} D_f(E) f(E) dE \quad (3)$$

$$p_t = \int_{-\infty}^{\infty} D_t(E) f(E) dE \quad (4)$$

$$f(E) = \{1 + \exp[(E_F - E + q\phi(x)) / k_B T]\}^{-1} \equiv \{1 + \exp[(E_F(x) - E) / k_B T]\}^{-1} \quad (5)$$

Here  $f(E)$  is the Fermi-Dirac (FD) distribution function,  $E_F$  is the Fermi energy level without external electric field, and  $E_F(x) = E_F + q\phi(x)$  is the quasi-Fermi energy level. There is no constant  $E_F(x)$  in a device under SCL conditions, but the separated  $E_F$  should be a constant.

It should be pointed out that although the same FD distribution  $f(E)$  is used in both Eqs. (3) and (4), Refs. [20, 21] show that the Einstein relationship is valid for organic semiconductors, this implies that the organic semiconductors should be nondegenerate,  $(E_F - E_v) \gg kT$ . Therefore, the position of  $E_F$  is near  $E_t$  and deviated from  $E_v$  in Fig. 1. The boundary conditions in Eqs. (16,17) shows that  $\varphi(x) > 0$ , so even under SCL conditions, the quasi-Fermi energy  $E_F(x)$  also satisfies the nondegenerate condition,  $(E_F(x) - E_v) \gg kT$ . This means that the free holes can be seen as non-degenerate, and the trapped holes should be treated as degenerate. The Fermi-Dirac distribution in Eq. (4) can and cannot be approximated by Boltzmann distribution as applied to free holes and trapped holes, respectively. And Eq. (3) for free holes can be simplified as following form

$$p_f = \int_{-\infty}^{\infty} D_f(E) \exp[(E - E_F - q\varphi(x)) / kT] dE \quad (6)$$

Defining the effective DOS

$$N_f = \int_{-\infty}^{\infty} D_f(E) \exp[(E - E_F) / kT] dE \quad (7)$$

the density of free holes can be expressed as

$$p_f = N_f \exp[(-q\varphi(x)) / kT] \quad (8)$$

Introducing dimensionless variable,  $y = (E - E_v) / \sigma\sqrt{2}$ , we can evaluate the integral in Eq. (7)

$$\int_{-\infty}^{\infty} \exp[-(E - E_v)^2 / 2\sigma^2] \exp[(E - E_v) / kT] dE = \sigma\sqrt{2\pi} \exp\left[\frac{\sigma^2}{(\sqrt{2}kT)^2}\right]$$

And obtain expression of effective DOS as follows

$$N_f = N_0 \exp[(E_v - E_F) / kT] \exp\left[\frac{\sigma^2}{2(kT)^2}\right] \quad (9)$$

where  $\sigma$  the standard deviation of the Gaussian distribution. Although the Fermi-Dirac (FD) distribution in Eq. (5) cannot be approximated by Boltzmann distribution as applied to trapped holes, we can reformulate it by using Eq. (8). Solving Fermi energy  $E_F$  from Eqs. (8) and substituting it into Eq. (5), we obtain

$$f(E) \approx \left\{1 + (N_f/p_f) \exp[(E_F - E)/k_B T]\right\}^{-1} \quad (10)$$

One situation easy misunderstanding is that to derive Eq. (8), the Fermi-Dirac distribution is approximated by a Boltzmann distribution and then, this result is substituted in the Fermi-Dirac statistics in Eq. (5) and arrives at Eq. (10). This treatment is correct, and we explain the reason in more detail. The original Fermi distribution Eq. (5) is applicable to both free and trapped holes. But the Boltzmann approximation in Eq. (8) merely is used to free holes. As the transformed Eq. (10) is applied to free holes, we may obtain the identity,  $p_f = p_f$ . So no contradiction there exists in Eq. (10).

Nicolai *et al.* [20, 21] pointed out that the trapped holes can be easily realized in program based on the discretization method of Gummel and Scharfetter [39, 40], if the  $D_t(E)$  for trapped holes being taken as the single trap model. Whereas, the Fermi integral in Eq. (4) with Gaussian DOS is not easy to realize [20, 21]. It is necessary to use the accurate approximation of the Gauss-Fermi integral recently reported by Paasch and Scheinert [41]. By using their approximation [41], the effect of Gaussianly distributed traps on the transport can be accessed. However, from Eq. (10), we can derive following expression

$$p_f(\partial f / \partial p_f) = \left\{1 + (N_v/p_f) \exp[(E_F - E)/k_B T]\right\}^{-2} (N_f/p_f) \exp[(E_F - E)/k_B T] \quad (11)$$

Substitution of Eq. (10) into Eq. (11) yields

$$p_f(\partial f / \partial p_f) = f^2(f^{-1} - 1) = f(1 - f) \quad (12)$$

Then the derivatives of trapped charges with respect to the free charges can be easily evaluated as

$$p_f(\partial p_t / \partial p_f) = (N_t / \sigma_t \sqrt{2\pi}) \int_{-\infty}^{\infty} \exp\left\{-\left[(E - E_t) / \sigma_t \sqrt{2}\right]^2\right\} f(E)[1 - f(E)] dE \quad (13)$$

By the combination of Eq. (13) with the discretization method of Gummel and Scharfetter [39, 40], the Gauss-Fermi integral can be easily and directly realized in program, and no need of the approximation of Paasch and Scheinert [41].

With trapped charges taken into account, the Poisson equation is as follows

$$\frac{d^2\varphi}{dx^2} = -\frac{q}{\varepsilon_r\varepsilon_0}(p_f + p_i) \quad (14)$$

Considering that the trapped charges don't contribute to current, and supposing a constant mobility, drift-diffusion equation takes following form

$$J = -q\mu_0 p_f \frac{\partial\varphi}{\partial x} - kT\mu_0 \frac{\partial p_f}{\partial x} \quad (15)$$

As solving Eqs. (14, 15), we need use Eqs. (4, 8, 10).

Assuming the thickness of organic layer is  $L$ , the left-side contact ( $x = 0$ ) can be seen as Ohmic with low potential barrier  $W_{\text{left}}$ . And the right-side contact ( $x = L$ ) can be seen as Schottky with high potential barrier  $W_{\text{right}}$ . The difference between right and left potential barriers,  $V_{bi} = W_{\text{right}} - W_{\text{left}}$ , just is the built-in potential in the devices. The boundary conditions for the Poisson equation is as follows [27]

$$\varphi(0) = W_{\text{left}} + V, \quad \varphi(L) = W_{\text{right}} \quad (16)$$

$$V - V_{bi} = \varphi(0) - \varphi(L) \quad (17)$$

As for the boundary conditions for the drift-diffusion equations, Neumann et al. [31, 32] have derived following equations

$$p_f(0) = N_f \exp\left[-\frac{W_{\text{left}}}{kT} - \frac{\varepsilon_r q l_{\text{left}}}{kT} F(0)\right] \quad (18a)$$

$$p_f(L) = N_f \exp\left[-\frac{W_{\text{right}}}{kT} + \frac{\varepsilon_r q l_{\text{right}}}{kT} F(L)\right] \quad (18b)$$

Where  $F(0)$  and  $F(L)$  are values of electric field at contacts,  $l$  is a characteristic length of electrodes

$$l = \sqrt{\frac{2\varepsilon_0 E_\infty}{3q^2 n_\infty}} \quad (19)$$

The typical values of parameters in Eq. (19) are as follows,  $n_\infty \approx 4\text{eV}$ ,  $E_\infty \approx 3 \times 10^{28} \text{ m}^{-3}$ , the value of  $l$  is about  $7.088 \times 10^{-11} \text{ m}$ . In the devices studied in this paper, the values of  $F(0)$  and  $F(L)$  are about  $10^3$  and  $10^7$  (V/m), respectively. The values of  $\varepsilon_r q l_{\text{left}} F(0)$  and  $\varepsilon_r q l_{\text{right}} F(L)$  are about  $10^{-6}$  and  $10^{-2}$  eV, respectively.

The second terms in exponential functions of Eq. (18) can be neglected as compared with the first terms.

And Eq. (18) can be simplified to following form [27]

$$p_f(0) = N_f \exp(-W_{left}/kT), \quad p_f(L) = N_f \exp(-W_{right}/kT) \quad (20)$$

These boundary conditions Eqs. (16, 20) have been used by Bruyn et al. [27].

Ahead of concrete calculations, it is necessary to explain our model goes beyond the suggestion of previous publications. At first, Nicolai et al. [20, 21] adopted the program in [3] of Koster et al., they didn't consider potential barriers at contacts, and adopted symmetric Ohmic contacts with  $W_{left} = W_{right}$ , as mentioned in last line of page 2 in [20]. But our calculations show that the asymmetric contacts with different barriers are very important to improve fitting quality of experimental J-V data. At second, Nicolai et al. [20, 21] didn't mention boundary conditions used for the drift-diffusion equations. At third, they didn't not use the non-degenerate condition for free holes, and didn't extract effective DOS as function of temperature. They also didn't extract temperature function of mobility. At fourth, they didn't derive relationships in Eqs. (11-13), they must use approximation of the Gauss-Fermi integral proposed by Paasch and Scheinert [41].

### 3. Analysis

Eqs. (4, 8, 10, 14, 15) show that the calculation of trap-limited currents requires a separation of the total carrier density into free ( $p_f$ ) and trapped ( $p_t$ ) carriers. We plot the ( $p_t - p_f$ ) relationship with different values of  $\sigma$  in Fig. 2. The figure also shows that the influence of  $\sigma$  to ( $p_t - p_f$ ) curves is very prominent. The  $p_t$  always is an increasing function of  $p_f$  and  $\sigma$ . The slopes of ( $p_t - p_f$ ) curves are large as  $p_f$  being low and small  $\sigma$ , the slopes decrease as  $p_f$  and  $\sigma$  increasing. The  $p_t$  would reach saturation at high  $p_f$ . There exists a cross point of  $p_f$  for all curves, at this value of  $p_f$ , all curves take the same value of  $p_t$ .

Now we give a qualitative explanation to increase of mobility and GER based on trapped charges. For simplicity, we just consider the single trap case. In terms of Eqs. (4, 10), if supposing single trap level  $E_t$ , the density of trapped charges can be expressed as

$$p_t = N_t f(E_t) = N_t \{1 + (N_f/p) \exp[(E_F - E_t)/k_B T]\}^{-1} \quad (21)$$

In the situation considering GER, it is not needed to divide the carriers into free and trapped types. We may introduce total density of carriers

$$p = p_f + p_t \quad (22)$$

the Poisson and DD equations can be reformulated by using  $p$

$$\frac{d^2 \phi}{dx^2} = -\frac{q}{\epsilon_r \epsilon_0} p \quad (23)$$

$$J = -qp\mu \frac{\partial \phi}{\partial x} - qD \frac{\partial p}{\partial x} \quad (24)$$

The substitution of Eq. (21) into Eq. (22) results in the quadratic equation for  $p_f$

$$p_f^2 - p_f(p - N_t - N_q) - pN_q = 0 \quad (25)$$

The solution is as follows

$$p_f = (1/2)(p - N_t - N_q) + (1/2)[(p - N_t - N_q)^2 + 4N_q p]^{1/2} \quad (26)$$

$$N_q = N_f \exp[(E_F - E_t)/k_B T] \quad (27)$$

Its derivative can be evaluated as

$$\frac{\partial p_f}{\partial x} = (1/2) \left\{ 1 + [(p - N_t - N_q)^2 + 4N_q p]^{-1/2} (p - N_t + N_q) \right\} \frac{\partial p}{\partial x} \equiv Q(p) \frac{\partial p}{\partial x} \quad (28)$$

If substituting Eqs. (26, 28) into Eqs. (14, 15), and comparing the resulting equation with Eq. (23, 24), we obtain the effective mobility and diffusion coefficient

$$\mu = (p_f/p)\mu_0, \quad D = \left( \frac{\partial p_f}{\partial x} \right) \left( \frac{\partial p}{\partial x} \right)^{-1} \left( \frac{kT}{q} \right) \mu_0 \quad (29)$$

$$\frac{D}{\mu} = \left( \frac{p}{p_f} \right) \left( \frac{\partial p_f}{\partial x} \right) \left( \frac{\partial p}{\partial x} \right)^{-1} \left( \frac{kT}{q} \right) = Q(p) \left( \frac{p}{p_f} \right) \left( \frac{kT}{q} \right) \quad (30)$$

It should be pointed out that trap-modulated mobilities were introduced decades ago [1,2,4, 23-26], although not within the Gaussian DOS leading to Eqs. (29), and there are many possibilities GERs, for example field-depend mobility [33-37].

Eq. (29) shows that although the mobility  $\mu_0$  in the original model in Eqs. (14, 15) is a constant, where the carriers being divided into free and trapped types, the effective mobility  $\mu$  and diffusion coefficient  $D$  in the transformed Eq. (24) become functions of density of carriers. In Fig. 3, we plot the relationships of  $\mu$  and  $D/\mu$  with  $p$ . The figure show that  $\mu$  is a increasing function of  $p$ , and the increase becomes more dramatic as the depth of traps increases. This tendency is in agreement with that of VM theory [4-7]. The VM theory doesn't divide the carriers as free and trapped, and express  $\mu$  as a function of density of carriers.

Based on the analysis, one may deduce following assumption that the trapped carriers is equivalent to the function of effective mobility as density of carriers, both factors cannot be considered at same time. The latest works of Zhang *et al.* [19] and Nicolai *et al.* [20, 21] also consider this situation. Since they consider trapped charges in their model [19-21], they treat mobility as a constant, and don't use the mobility model of Pasveer *et al.* [8] which treat mobility as function of density of carriers and electric field. But both authors belong to same research group led by Blom [8, 19-21].

Fig. 3 also shows that the ratio of  $D/\mu$  indeed deviating from the ER value  $kT/q$ , and the GER appears. But the ratio also is different from the one in previous references [33-35], which the GER is due to degenerate effect of carriers. Since the viewpoint on GER is controversial in literature [33-36], and the latest experiment [37] supports the ER for free carriers, so the theoretical frame dividing carriers into free and trapped types is consistent with the experiment [37].

The model of Nicolai *et al.* [20, 21] doesn't consider the asymmetric barriers at contacts, and adopted symmetric Ohmic contacts with  $W_{left} = W_{right}$  [20]. In our calculations, it is shown that the potential barriers have severe impact on the shape of  $J$ - $V$  curves. In Fig. 4 we plot several  $J$ - $V$  curves with different values of  $W_{left}$  and  $W_{right}$ . The figure shows that if keeping  $W_{left}$  as constant and increasing  $W_{right}$  the  $J$ - $V$  curves would dramatically bend down at low voltage side. If keeping  $W_{right}$  as constant and increasing  $W_{left}$  the  $J$ - $V$  curves would move down and the slope also slightly decreases. So it is necessary to adjust values of  $W_{left}$  and  $W_{right}$  to fit shapes of  $J$ - $V$  curves.

#### 4. Application to devices

Now we apply above Gaussian model to polymer layers of poly[4'-(3,7-dimethyloctyloxy)-1,1'-biphenylene-2,5-vinylene] (NRS-PPV), poly(2-methoxy-5-(3',7'-dimethyloctyloxy)-p-phenylene-vinylene) (OC<sub>1</sub>C<sub>10</sub>-PPV) [8,10], and poly(3-hexylthiophene) (P3HT) [5,42], with thickness  $L=560$  nm, 275 nm and 95 nm respectively. In figures 5-7, we plot  $J$ - $V$  curves for the three materials with comparison with experimental points. The three figures show that the agreement of theoretical curves with experimental  $J$ - $V$  points is fairly good. For the three devices studied in this work, the agreement is quantitative for every isothermal line, not only the shapes and slopes from low to high voltage ranges, but also the values of current at every point within wide varying ranges, from  $10^{-6}\sim 1$ ,  $10^{-5}\sim 1$  and  $10^{-19}\sim 1$  A/m<sup>2</sup> for NRS-PPV, OC<sub>1</sub>C<sub>10</sub>-PPV and P3HT devices, respectively. Because the works of Nicolai *et al.* [20, 21] don't consider non-symmetric barriers at contacts, so they merely obtain qualitative agreement between theoretical results and experimental data. As compared with the works of Nicolai *et al.* [20, 21], it can be seen that the non-symmetric barriers are important factor for arrival of quantitative agreement between theoretical results and experimental data.

Nicolai et al. [20, 21] extracted parameters for the three materials as follows,  $\sigma \sim 0.1$  eV,  $N_t \sim (1.3 \times 10^{23} - 4.0 \times 10^{23}) \text{ m}^{-3}$ ,  $(E_t - E_v) \sim 0.6$  eV. Although they don't analyze variation of parameters with temperature, they postulate that the electron traps have a common origin, and is most likely related to hydrated oxygen complexes. However, analysis of variation of parameters with temperature is very important to improve the internal consistency of a theoretical model. Therefore, we list all parameters optimized in Tables 1 and 2. Our modified model yields that  $\sigma \sim (0.055 - 0.15)$  eV,  $N_t \sim (7.5 \times 10^{22} - 7.6 \times 10^{24}) \text{ m}^{-3}$ ,  $(E_{tF} = E_t - E_F) \sim 0.2$  eV. The dispersion of  $N_t$  is not in line with the postulation of Nicolai et al. [20, 21]. The positive value of  $E_{tF}$  means that the position of traps is higher than the Fermi energy  $E_F$ . Table 1 also shows that the values of  $W_{left}$  and  $W_{right}$  are non-symmetric, with  $W_{right} > W_{left}$  and the built-in potential  $V_{bi} = W_{right} - W_{left}$  in the devices is positive.

We may further analyze variations of  $N_f$  and  $\mu_0$  with temperature. We can fit  $N_f$  by using Eq. (8) and determine characteristic energies of  $E_{vF} = E_v - E_F$  and  $\sigma$ . The  $\mu_0$  can be fitted by using following non-Arrhenius expression

$$\mu_0 = \mu_{00} \exp\left[\frac{\Delta}{kT} + \lambda\left(\frac{\Delta}{kT}\right)^2\right] \quad (31)$$

with three regression coefficients  $\mu_{00}$ ,  $\Delta$  and  $\lambda$ . The fitted curves are compared with data points in Fig. 8. The figure shows that the agreement is satisfactory. The determined parameters for  $N_f$  and  $\mu_0$  are listed in Table 3. The values of  $E_{vF} = E_v - E_F$  always are negative, which means that the Fermi energy  $E_F$  always is higher than the valence level  $E_v$ . The free holes indeed are non-degenerate, and the formulae for free holes in Eqs. (8, 9) are reasonable. We can calculate  $E_{tv}$  in terms of the relationship,  $E_{tv} = E_t - E_v = (E_t - E_F) - (E_v - E_F) = E_{tF} - E_{vF}$ . The results are about 0.22, 0.44 and 0.45 for NRS, OCC and P3HT, respectively. This is within error range of Nicolai et al., their results are about 0.6 eV. So our results for  $E_{tv}$

are in line with that of Nicolai et al., and support the assumption that the electron traps have a common origin, and is most likely related to hydrated oxygen complexes.

## 5. Conclusion

In this work, we analyze variations of the density of trapped carriers with the density of free carriers, the effective mobility and ratio of diffusion coefficient to effective mobility with the density of trapped carriers. It is shown that the density of trapped carriers is a dramatically increasing function of the density of free carriers at low density, and tends saturation at high density. The density of trapped carriers always is increasing function of the density of trapped carriers, and the slope dramatically increases as high density of trapped carriers. Although the ratio of diffusion coefficient to effective mobility is the Einstein type for free carriers, the ratio for total carriers is the non-Einstein type, and is an increasing function of the density of trapped carriers at low density, decreasing function at high density. This explains recent argument about Einstein or non-Einstein types.

We emphasize the importance of non-symmetric barriers at contacts to quantitatively describe the current-voltage relationships of typical organic layers sandwiched in two metallic electrodes. It is shown that slopes of current-voltage curves at low bias are very sensitive to the values of right barriers. The slopes in all bias are sensitive to the values of left barriers, and would increase as the left barrier decreasing.

As applying the modified model to three typical devices with organic NRS-PPV, OCC-PPV and P3HT layers, we obtain excellent agreement between theoretical results and experimental data. Evident improvement can be seen as compared with the qualitative agreement of Nicolai et al. [20, 21] The

extracted main parameters of materials are within error range of Nicolai et al., and support the assumption that the electron traps have a common origin.

### Acknowledgments

This work was supported by the Program for Excellent Talents of Sichuan Province of China under Grant No 2011JQ0053, and the Science and Technology Foundation of State Key Laboratory for Shock Wave and Detonation Physics under Grant No. 9140C670103120C6702.

### References

- [1] P. S. Davids, I. H. Campbell, and D. L. Smith. Device model for single carrier organic diodes, *J. Appl. Phys.* 82, 6319 (1997).
- [2] B. K. Crone, P. S. Davids, I. H. Campbell, and D. L. Smith. Device model investigation of bilayer organic light emitting diodes, *J. Appl. Phys.* 87, 19742 (2000).
- [3] L. J. A. Koster, E. C. P. Smits, V. D. Mihailetschi, and P. W. M. Blom. Device model for the operation of polymer/fullerene bulk heterojunction solar cells, *Phys. Rev. B* 72, 085205 (2005).
- [4] M. C. J. M. Vissenberg and M. Matters, Theory of the field-effect mobility in amorphous organic transistors, *Phys. Rev. B* 57, 12964 (1998).
- [5] C. Tanase, E. J. Meijer, P.W. M. Blom, and D. M. de Leeuw, Unification of the hole transport in polymeric field-effect transistors and light-emitting diodes, *Phys. Rev. Lett.* 91, 216601 (2003).
- [6] M. Kiguchi, M. Nakayama, T. Shimada, K. Saiki, Electric-field-induced charge injection or exhaustion in organic thin film transistor, *Phys. Rev. B* 71, 035332 (2005).
- [7] F. Torricelli, K. O'Neill, G. H. Gelinck, K. Myny, J. Genoe, and E. Cantatore, Charge transport in organic transistors accounting for a wide distribution of carrier energies - Part II: TFT modeling, *IEEE Trans. Electron Dev.* 59, 1520 (2012).

- [8] W.F. Pasveer, J. Cottaar, C. Tanase, R. Coehoorn, P.A. Bobbert, P.W.M. Blom, D.M. de Leeuw, M.A.J. Michels, Unified description of charge-carrier mobilities in disordered semiconducting polymers, *Phys. Rev. Lett.* 94, 206601 (2005).
- [9] J. Cottaar, P.A. Bobbert, Calculating charge-carrier mobilities in disordered semiconducting polymers: Mean field and beyond, *Phys. Rev. B* 74, 115204 (2006).
- [10] F. Torricelli, D. Zappa, L. Colalongo, Space-charge-limited current in organic light emitting diodes, *Appl. Phys. Lett.* 96, 113304 (2010).
- [11] S.L.M. van Mensfoort, R. Coehoorn, Effect of Gaussian disorder on the voltage dependence of the current density in sandwich-type devices based on organic semiconductors, *Phys. Rev. B* 78, 085207 (2008).
- [12] J. Li, J.X. Sun, Ch. Zhao, Improved expression of charge-carrier mobility in disordered semiconducting polymers considering dependence on temperature, electric field and charge-carrier density, *Synth. Met.* 159, 1915 (2009).
- [13] B. Xue, J.X. Sun, K. Yang, Improvement of unified mobility model with analytic current-voltage expression for organic diodes, *J. Macromol. Sci. B* 51, 1415 (2012).
- [14] J. Zhou, Y.C. Zhou, J.M. Zhao, C.Q. Wu, X.M. Ding, X.Y. Hou, Carrier density dependence of mobility in organic solids: A Monte Carlo simulation, *Phys. Rev. B* 75, 153201 (2007).
- [15] V. Coropceanu, J. Cornil, D. A. da Silva Filho, Y. Olivier, R. Silbey, and J. L. Brédas. Charge transport in organic semiconductors, *Chem. Rev.* 107, 926 (2007).
- [16] R. Coehoorn and P. A. Bobbert, Effects of Gaussian disorder on charge carrier transport and recombination in organic semiconductors, *Phys. Status Solidi A* 209, 2354 (2012).
- [17] Bäessler H., Köhler A. Charge transport in organic semiconductors, *Top Curr Chem.* 312, 1 (2012).
- [18] Jason D. Myers, J. G. Xue. Organic semiconductors and their applications in photovoltaic devices, *Polymer Rev.* 52, 1 (2012).
- [19] Y. Zhang, B. de Boer, and P.W. M. Blom, Trap-free electron transport in poly(p-phenylene vinylene) by deactivation of traps with n-type doping, *Phys. Rev. B* 81, 085201 (2010).
- [20] H.T. Nicolai, M.M. Mandoc, P.W.M. Blom, Electron traps in semiconducting polymers: Exponential versus Gaussian trap distribution, *Phys. Rev. B* 83, 195204 (2011).

- [21] H.T. Nicolai, M. Kuik, G.A.H. Wetzelaer, B. de Boer, C. Campbell, C. Risko, J.L. Brédas, P.W.M. Blom, Unification of trap-limited electron transport in semiconducting polymers, *Nature Mater. (Lond.)* 11, 882 (2012).
- [22] I. Lange, J. C. Blakesley, J. Frisch, A. Vollmer, N. Koch, and D. Neher. Band bending in conjugated polymer layers, *Phys. Rev. Lett.* 106, 216402 (2011).
- [23] J. Cottaar, L. J. A. Koster, R. Coehoorn, and P. A. Bobbert. Scaling theory for percolative charge transport in disordered molecular semiconductors, *Phys. Rev. Lett.* 107, 136601 (2012).
- [24] J. Cottaar, R. Coehoorn, and P. A. Bobbert. Scaling theory for percolative charge transport in molecular semiconductors: correlated versus uncorrelated energetic disorder, *Phys. Rev. B* 85, 245205 (2012).
- [25] J. O. Oelerich, D. Huemmer, and S. D. Baranovskii. How to find out the density of states in disordered organic semiconductors, *Phys. Rev. Lett.* 108, 226403 (2012).
- [26] I. I. Fishchuk, A. Kadashchuk, S. T. Hoffmann, S. Athanasopoulos, J. Genoe, H. Bässler, and A. Köhler. Unified description for hopping transport in organic semiconductors including both energetic disorder and polaronic contributions. *Phys. Rev. B* 88, 125202 (2013).
- [27] P. de Bruyn, A. H. P. van Rest, G. A. H. Wetzelaer, D. M. de Leeuw, and P.W. M. Blom. Diffusion-limited current in organic metal-insulator-metal diodes. *Phys. Rev. Lett.* 111, 186801 (2013).
- [28] L. W. Chen, R. Ludeke, X. D. Cui, A. G. Schrott, C. R. Kagan, and L. E. Brus. Electrostatic field and partial fermi level pinning at the Pentacene-SiO<sub>2</sub> interface, *J. Phys. Chem. B* 109, 1834 (2005).
- [29] S. Yogeve, R. Matsubara, M. Nakamura, U. Zschieschang, H. Klauk, and Y. Rosenwaks. Fermi level pinning by gap states in organic semiconductors, *Phys. Rev. Lett.* 110, 036803 (2013).
- [30] M. Oehzelt, N. Koch, and G. Heimel. Organic semiconductor density of states controls the energy level alignment at electrode interfaces, *Nature (Comm.)*, 2014, DOI: 10.1038/ncomms5174
- [31] F. Neumann, Y. A. Genenko, C. Melzer, and H. von Seggern. Self-consistent theory of unipolar charge-carrier injection in metal/insulator/metal systems, *J. Appl. Phys.* 100, 084511 (2006).
- [32] F. Neumann, Y. A. Genenko, C. Melzer, S. V. Yampolskii, and H. von Seggern. Self-consistent analytical solution of a problem of charge-carrier injection at a conductor/insulator interface, *Phys. Rev. B* 75, 205322 (2007).
- [33] Y. Roichman, N. Tessler. Generalized Einstein relation for disordered semiconductors—implications for device performance, *Appl. Phys. Lett.* 80, 1948 (2002).

- [34] Y.Q. Peng, J.H. Yang, F.P. Lu et al. Einstein relation in chemically doped organic semiconductors, *Appl. Phys. A* 86, 225 (2007).
- [35] A. Das, A. Khan. Mobility–diffusivity relationship for heavily doped organic semiconductors, *Appl. Phys. A* 93, 527 (2008).
- [36] X. H. Lu, J. X. Sun, Y. Guo, Da Zhang. Potential-Dependent Generalized Einstein Relation in Disordered Organic Semiconductors, *Chin. Phys. Lett.* 26, 087202 (2009)
- [37] F. Neumann, Y.A. Genenko, H. von Seggern. The Einstein relation in systems with trap-controlled transport, *J. Appl. Phys.* 99, 013704 (2006).
- [38] G.A.H. Wetzelaer, L.J.A. Koster, P.W.M. Blom. Validity of the einstein relation in disordered organic semiconductors, *Phys. Rev. Lett.* 107, 066605 (2011).
- [39] H.K. Gummel, A self-consistent iterative scheme for one-dimensional steady state transistor calculations, *IEEE Trans. Electron Devices* 11, 455 (1964).
- [40] D.L. Scharfetter, H.K. Gummel, Large-signal analysis of a silicon Read diode oscillator, *IEEE Trans. Electron Devices* 16, 64 (1969).
- [41] G. Paasch and S. Scheinert, Charge carrier density of organics with Gaussian density of states: Analytical approximation for the Gauss–Fermi integral, *J. Appl. Phys.* 107, 104501 (2010).
- [42] N. I. Craciun, J. Wildeman, and P.W. M. Blom, Universal arrhenius temperature activated charge transport in diodes from disordered organic semiconductors, *Phys. Rev. Lett.* 100, 056601 (2008).

**Table 1** Temperature-independent parameters of double Gaussian model with non-symmetric potential barriers at contacts optimized by fitting J-V data for NRS, OCC [8, 10] and P3HT [5, 42] organic diodes.

**Table 2** Temperature-dependent parameters  $N_f$  and  $\mu_0$  of double Gaussian model with non-symmetric potential barriers at contacts optimized by fitting J-V data for NRS, OCC [8, 10] and P3HT [5, 42] organic diodes.

**Table 3** Temperature-independent parameters for functions  $N_f(T)$  and  $\mu_0(T)$  determined by fitting data in Table 1.

**Fig. 1** (color online). Schematic diagram of energy-band model proposed in this paper.

**Fig. 2** (color online). Schematic diagram for the  $(p_t - p_f)$  relationship calculated by using Eqs. (4, 10) at 300 K, with  $N_f = 10^{26}/\text{m}^3$ ,  $N_t = 10^{23}/\text{m}^3$ ,  $E_{tF} = 0.3$  eV, and with different values of  $\sigma_t$ ,  $\sigma_t = 0, 0.05, 0.1, 0.15, 0.2$  eV, respectively. The calculations in this figure don't involve the Gaussian width  $\sigma$  of free holes.

**Fig. 3** (color online). The qualitative  $(\mu - p)$  and  $(D/\mu - p)$  relationships calculated by using Eqs. (26-30) at 300 K, with  $N_f = 10^{26}/\text{m}^3$ ,  $N_t = 10^{23}/\text{m}^3$ ,  $E_{tF} = 0.2$  eV (solid lines) and 0.3 eV (dashed lines), and with  $\sigma_t = 0$  eV. The calculations in this figure don't involve the Gaussian width  $\sigma$  of free holes.

**Fig. 4** (color online). The  $J$ - $V$  curves calculated at 300 K, with  $\mu_0 = 2 \times 10^{-10}$  m<sup>2</sup>/Vs,  $N_t = 2 \times 10^{22}/\text{m}^3$ ,  $\sigma = 0.1$  eV, and  $E_{tF} = 0.22$  eV. (a)  $W_{left} = 0.1$  eV, and  $W_{right} = (0.1, 0.3, 0.5, 0.7, 0.9)$  eV. (b)  $W_{right} = 0.1$  eV, and  $W_{left} = (0.1, 0.3, 0.5, 0.7, 0.9)$  eV.

**Fig. 5** (color online). Experimental (symbols) [8, 10] and theoretical (lines)  $J$ - $V$  curves of a NRS-PPV hole only diode, with thickness  $L=560$  nm and at different temperatures.

**Fig. 6** (color online). Experimental (symbols) [8, 10] and theoretical (lines)  $J$ - $V$  curves of a OC<sub>1</sub>C<sub>10</sub>-PPV hole only diode, with thickness  $L=275$  nm and at different temperatures.

**Fig. 7** (color online). Experimental (symbols) [5, 42] and theoretical (lines)  $J$ - $V$  curves of a P3HT hole only diode, with thickness  $L=95$  nm and at different temperatures.

**Fig. 8** (color online). Variations of  $N_f(T)$  and  $\mu_0(T)$  with temperature. Symbols are data listed in Table 2, and lines are smoothed curves by using Eq. (9) and Eq. (31), respectively.

Table 1

	NRS	OCC	P3HT
$\sigma_i$ (eV)	0.055	0.1285	0.15
$N_i$ (m <sup>-3</sup> )	7.55E22	1.3E24	7.6E24
$E_{iF}$ (eV)	0.2	0.11	0.235
$W_{left}$ (eV)	0.1	0.375	0.28
$W_{right}$ (eV)	1.01	0.578	1.2

Table 2

	$T$ (K)	233	252	272	298	
NRS	$N_f$ (m <sup>-3</sup> )	2.12E25	2.2E25	2.3E25	2.4E25	
	$\mu_0$ (m <sup>2</sup> /Vs)	1.4E-11	2.75E-11	3.9E-11	8.5E-11	
	$T$ (K)	235	255	275	293	
OCC	$N_f$ (m <sup>-3</sup> )	2.7E26	2.8E26	3.0E26	3.5E26	
	$\mu_0$ (m <sup>2</sup> /Vs)	1.1E-7	1.2E-7	1.4E-7	1.5E-7	
	$T$ (K)	215	235	255	275	294
P3HT	$N_f$ (m <sup>-3</sup> )	3.0E18	1.7E19	2.9E19	3.5E19	1.0E20
	$\mu_0$ (m <sup>2</sup> /Vs)	2.2E-9	2.2E-8	1.3E-6	2.0E-5	2.0E-4

Table 3

	NRS	OCC	P3HT
$N_0$ (m <sup>-3</sup> )	4.6756E25	8.5742E29	4.6121E23
$E_{vF}$ (eV)	-0.0214	-0.3350	-0.2158
$\sigma$ (eV)	0.0149	0.0834	0.00
$\mu_{00}$ (m <sup>2</sup> /Vs)	2.2073E-6	2.6554E-6	3.8970E023
$\Delta$ (eV)	-0.3411	-0.1037	-2.1517
$\lambda$	0.0175	0.0737	0.0031

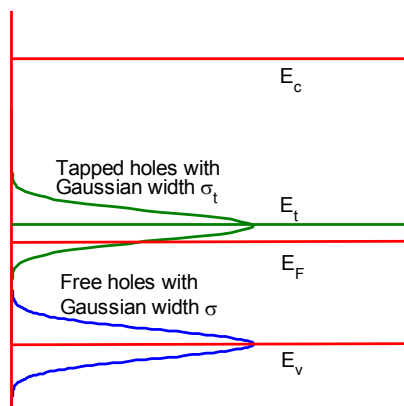


Fig. 1

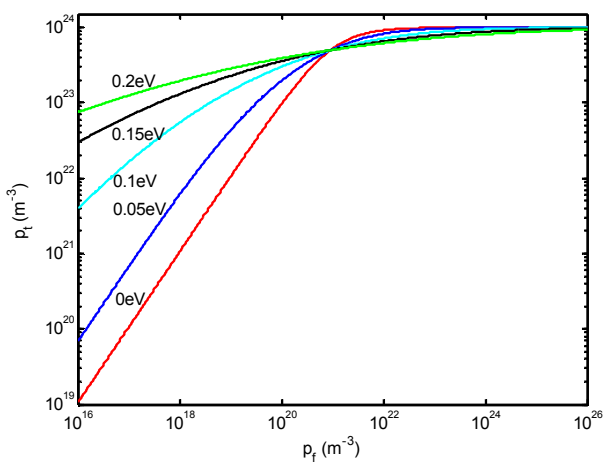


Fig. 2

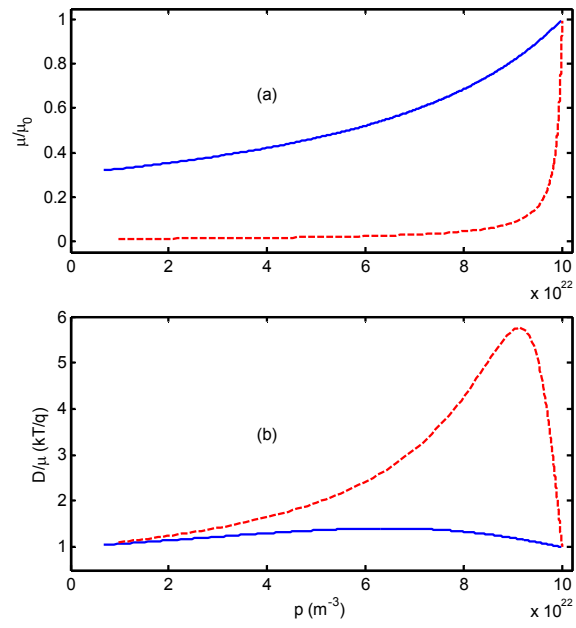


Fig. 3

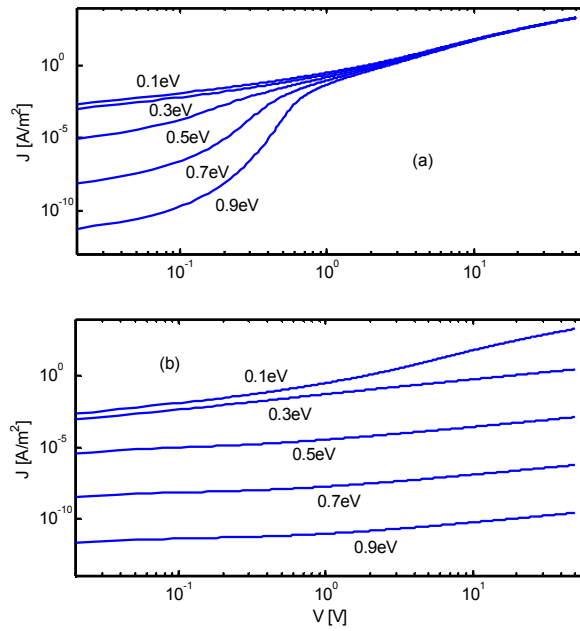


Fig. 4

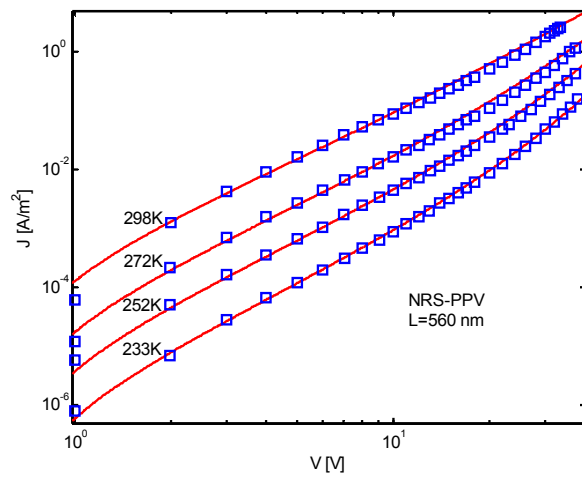


Fig. 5

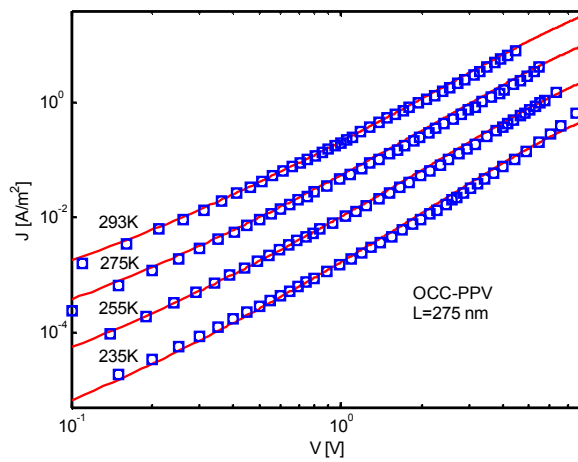


Fig. 6

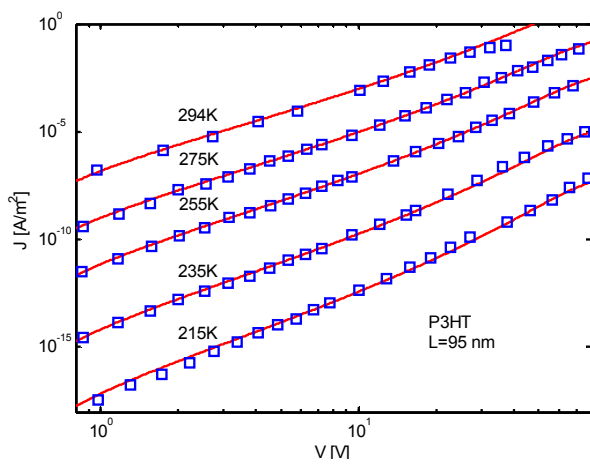


Fig. 7

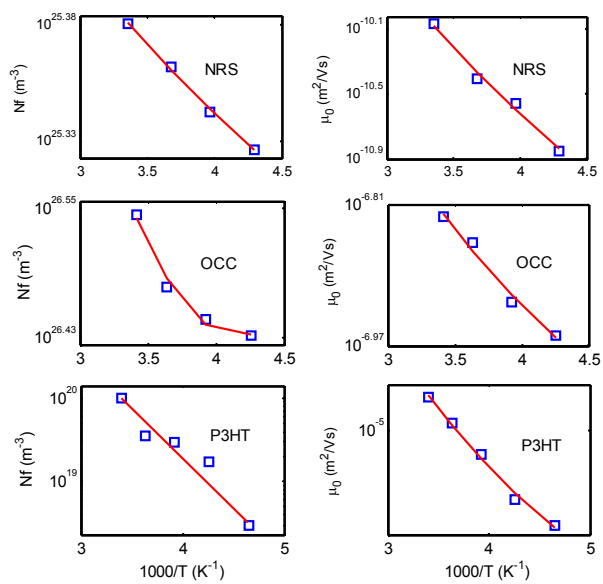


Fig. 8